

Stefan Funk for the H.E.S.S. collaboration

Status of Identification of VHE γ -ray sources

the date of receipt and acceptance should be inserted later

Abstract Keywords RX J1713.7–3946 · HESS J1825–137 · HESS J1813–178 · Gamma-rays · H.E.S.S. · Source Identification

PACS First · Second · More

With the recent advances made by Cherenkov telescopes such as H.E.S.S. the field of very high-energy (VHE) γ -ray astronomy has recently entered a new era in which for the first time populations of Galactic sources such as e.g. Pulsar wind nebulae (PWNe) or Supernova remnants (SNRs) can be studied. However, while some of the new sources can be associated by positional coincidence as well as by consistent multi-wavelength data to a known counterpart at other wavelengths, most of the sources remain not finally identified. In the following, the population of Galactic H.E.S.S. sources will be used to demonstrate the status of the identifications, to classify them into categories according to this status and to point out outstanding problems.

1 Introduction

A systematic survey of the inner part of the Galaxy performed by the H.E.S.S. Cherenkov telescope system has revealed a number of previously unknown sources of VHE gamma-rays above 100 GeV [1] [2]. While in terms of a population approach the sources can be described by common properties like generally rather hard energy spectra (photon index ~ 2.3) or a rather narrow distribution in Galactic latitude (rms of $\sim 0.3^\circ$) the counterpart identification calls for an individual study of these objects. An unambiguous counterpart identifica-

Table 1 Categories into which the gamma-ray sources will be classified in the following sections.

	Matching position/ morphology	Viable emission mechanism	Consistent MWL picture
A	yes	yes	yes
B	no	yes	yes
C	yes	yes	no
D	no	no	no

tion of these (initially) unidentified H.E.S.S. sources requires **(i) spatial and ideally also morphological coincidence**, **(ii) a viable gamma-ray emission mechanism** for the object, and **(iii) a consistent multi-wavelength behaviour** matching the suggested identification and the particle distribution within the source. The H.E.S.S. sources can be classified according to their confidence in identification with known astrophysical objects following the three requirements given above. Table 1 summarises the categories. **Category A** comprises sources for which the positional and/or morphological match (in case of an extended source) with a counterpart source is excellent and the emission processes can be modelled to provide a consistent picture describing the multi-frequency data. For these sources the association is beyond doubt. For **Category B** sources the emission mechanisms can be consistently modelled, however these sources show a less convincing positional and/or morphological match with the potential counterpart. **Category C** sources on the other hand have a good positional counterpart, they show however a non-consistent multi-wavelength picture, being it because of insufficient data at other wavebands, being it because of a not fully understood emission mechanism. For **Category D** sources no counterpart candidate exists, these are the classical *unidentified sources*. In the following I will describe examples for sources belonging to each of the 4 categories. The description will focus on Galactic gamma-ray sources, since for extragalactic objects the counterpart

Stefan Funk
Kavli Institute for Particle Astrophysics and Cosmology,
Stanford University, 2575 Sand Hill Road, PO Box 0029,
Stanford, CA-94025 USA
Tel.: +1-650-926-8979
Fax: +1-650-926-5566
E-mail: Stefan.Funk@slac.stanford.edu / Accepted: date

identification in the VHE gamma-ray regime has (so far) turned out to be rather unproblematic.

2 Category A - Sources with an established counterpart

Two classes of sources can be distinguished for which a counterpart to the VHE gamma-ray source has been established: **a) point sources with a convincing positional match** and **b) extended sources with a convincing positional and morphological match**. For these objects with a firm counterpart, having established the positional coincidence, the aim for these objects is to fully understand the details of the multi-frequency photon spectrum and to investigate the emission mechanisms generating this photon spectrum. One important question in the VHE gamma-ray regime is for example whether the gamma-ray emission is generated by Inverse Compton scattering of ultra-relativistic electrons on photon fields like the Cosmic microwave background (CMBR) or by pion-decay produced in proton-proton interactions, that is whether the gamma-ray emission has leptonic or hadronic origin. These two scenarios can not be directly distinguished from the gamma-ray data alone, but have to be separated by modelling the parent population of particles responsible for the emission. For any source identification it should be mentioned that the good angular resolution of VHE Cherenkov instruments (typically of the order of 0.1° per event) as well as the very low level of the diffuse gamma-ray background at energies above 100 GeV helps against source confusion. Source confusion was a problem that EGRET [3] strongly had to face, especially in observations in the Galactic plane where both the density of sources and the level of the diffuse gamma-ray background was higher. The upcoming GLAST satellite measuring in the regime between 100 MeV to several hundreds of GeV will have the advantage of an improved angular resolution ($\sim 0.4^\circ$ at 1 GeV) over EGRET but will also be susceptible to any systematic uncertainties in modelling the diffuse gamma-ray flux from cosmic ray interactions with interstellar material. The best-established example for a **point-source with a convincing positional match** is the Crab Nebula [4], which is frequently used as a calibration source in VHE γ -ray astronomy. In order to establish a positional correlation with a gamma-ray point-source, it has to be tested whether the nominal position of the counterpart candidate is within the statistical and systematic error limits of the reconstructed position of the gamma-ray emission region (for the Crab Nebula, the statistical error on the reconstructed position of the gamma-ray emission is $5''$, the systematic error of the order of $20''$). Other objects of this class, where a positional counterpart to a point-like gamma-ray emission has been established are the newly discovered gamma-ray microquasars LS 5039 [5] [6] and LSI+61 303 [7] or

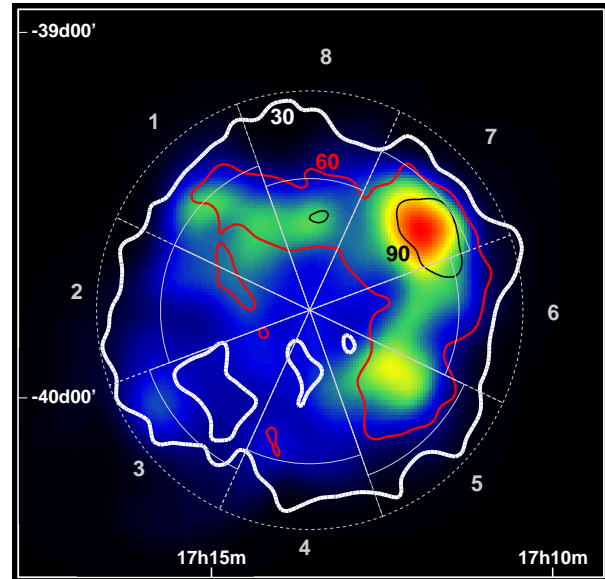


Fig. 1 ASCA x-ray image of RX J1713.7–3946, overlaid with smoothed and acceptance-corrected H.E.S.S. gamma-ray image contours linearly spaced at the level of 30, 60 and 90 counts. The ASCA image was smoothed to match the H.E.S.S. point-spread function for ease of comparison.

the composite PWN G0.9+0.1 [8]. A further strengthening of the proposed association can be established if additionally (as in the case of LS 5039) a correlated periodicity or variability between the gamma-ray source and the counterpart source can be detected (LS 5039 shows a modulation in the gamma-ray data that matches the orbital frequency of the binary system as discussed by deNaurois et al. in this proceedings).

The best established example for an **extended source with a convincing morphological match** is the Supernova remnant (SNR) RX J1713.7–3946 [9] [10] (and also see Lemoine-Gourmard et al. in this proceedings) showing a striking correlation of the gamma-ray emission to X-rays as e.g. measured by the ASCA satellite (correlation coefficient: $\sim 80\%$). From the morphological match, the association of the gamma-ray source with the Supernova remnant is beyond doubt and can be regarded as a firm association. Another object of this class is the Supernova remnant RX J0852.0–4622 (Vela Jr.) showing also a high degree of correlation between the gamma-ray and X-ray emission [11]. Other objects of this class are the PWNe MSH–15–52 [12] and Vela X [13].

In terms of modelling the multi-frequency emission from these objects where a firm counterpart has been established, the Crab Nebula can again serve as an excellent example how the outstanding coverage in wavebands from radio to VHE γ -rays can help to consistently describe the emission mechanism in this object and to derive important parameters like the strength of the magnetic field responsible for the synchrotron emission. For the microquasar LS 5039 as well as for the extended gamma-ray emission from the Supernova rem-

nants RX J1713.7–3946 and RX J0852.0–4622, there is not yet a unique solution to describe the multi-frequency data and the gamma-ray emission can be explained both in terms of a leptonic emission mechanism generated by Inverse Compton scattering as well as in terms of a hadronic scenario where the gamma-ray emission is generated by the decay of neutral pions.

3 Category B - Sources with a less convincing positional or morphological match

The best example for members of this class are the newly discovered gamma-ray sources, which seem to belong to the so-called *offset Pulsar wind nebulae*. These objects, for which Vela X [13] is the archetypal example show an extended emission around an energetic pulsar. The offset morphology is thought to arise from an anisotropy in the interstellar material surrounding the pulsar, that prevents the symmetric expansion of the PWN in one direction and shifts the emission to the other direction (see e.g. [14] for a hydro-dynamical simulation and discussion of this effect). The gamma-ray emission in these objects is generated by Inverse Compton scattering of relativistic electrons accelerated in the termination shock of the PWN. The gamma-ray sources that could possibly be explained in this framework are typically extended and their emission region overlaps with energetic pulsars (energetic enough to explain the gamma-ray flux by their spindown power) and that very importantly also show evidence for an X-ray PWN. Apart from Vela X and MSH–15–52, the gamma-ray emission of the PWN HESS J1825–137 [15] [16], possibly powered by the energetic pulsar PSR J1826–1334 can be used to illustrate the properties of this class of objects. This object has been observed by H.E.S.S. in a very deep observation of ~ 67 hours, due to its proximity to the microquasar LS 5039 (at a distance of $\sim 1^\circ$). It was known to be a PWN candidate also in VHE gamma-rays since through XMM-Newton X-ray observations of PSR J1826–1334 [17] established an offset X-ray PWN extending asymmetrically $\sim 5''$ to the south of the pulsar. The asymmetric nature of the PWN as well as CO data that show a dense molecular cloud to the north of PSR J1826–1334 [18] support the picture described above in which dense material to the north shifts the PWN emission to the south.

The H.E.S.S. detected gamma-ray emission similarly shows an asymmetric emission extending to the south of the pulsar, however on a completely different scale than the X-ray emission (the X-ray emission extends $5''$, whereas the gamma-ray emission extends $\sim 1^\circ$ to the south). This at first glance prevents a direct identification as a counterpart, since the morphology can not be matched between X-rays and gamma-rays. However, modelling the emission mechanism and taking into account the different loss timescales of the gamma-ray and X-ray emitting electrons the different scale of the emis-

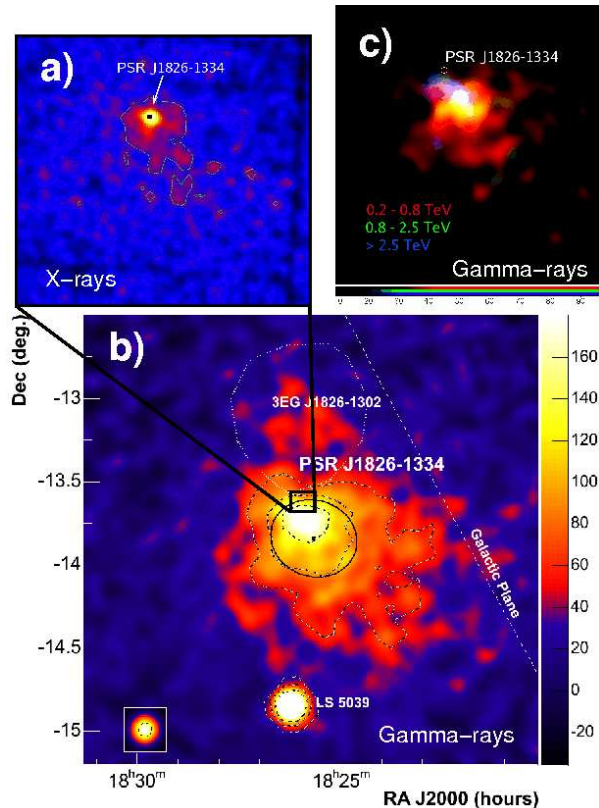


Fig. 2 a) XMM-Newton X-ray image in the energy range between 2 and 12 keV of the small region ($7' \times 7'$) surrounding PSR J1826–1334. It can be seen, that the X-ray emission shows an asymmetric diffuse emission extending to the south of the pulsar. b) H.E.S.S. gamma-ray excess image of the region surrounding HESS J1825–137 and the energetic pulsar PSR J1826–1334 (white triangle). The image has been smoothed with a Gaussian of radius $2.5'$ and has been corrected for the changing acceptance across the field. The inset in the bottom left corner shows the PSF of the data set (smoothed in the same way as the excess map). The dashed black and white contours are linearly spaced and denote the 5σ , 10σ and 15σ significance levels. The best fit position of HESS J1825–137 is marked with a black square, the best extension and position angle by a black ellipse. Also shown (dotted white) is the 95% positional confidence contour of the unidentified EGRET source 3EG J1826–1302. The bright point-source to the south of HESS J1825–137 is the microquasar LS 5039. c) Three-colour image, showing the gamma-ray emission as shown in panel b), with different colours, denoting the gamma-ray emission in different energy bands, symbolising the changing morphology even in the gamma-ray band alone. More details can be found in the text and in [16].

sion regions can be plausibly explained in the following way: for a typical magnetic field of $10 \mu\text{G}$ (as also suggested from the X-ray data), 1 keV X-rays are generated by ~ 50 TeV electrons, whereas 100 GeV gamma-rays are generated by ~ 1 TeV electrons. The gamma-rays are therefore generated by lower energy electrons than the X-rays and the different scales of the emission regions could be due to faster loss times of the higher energetic synchrotron emitting electrons. This picture is

further supported by the fact, that also in the gamma-ray regime on its own, a decrease in size with increasing energy can be established as shown in [16] and illustrated in Figure 2.

If this picture is correct and the X-ray and gamma-ray sources are associated, then the different morphologies in these two wavebands (i.e. the different angular scales) can be explained in a consistent picture. Therefore these two sources can possibly be associated, even though there is no direct morphological match. It should be noted, that in order to establish the association as a firm counterpart, more multi-frequency data are needed that confirm this picture. Also it should be mentioned, that this source generates a new template for a large number of other extended gamma-ray sources found close to energetic pulsars. However, in the case of HESS J1825–137 there are two striking arguments that further substantiate the association: a) the asymmetric X-ray PWN found by XMM and b) the changing morphology found by H.E.S.S. in the gamma-ray data. If these two properties had not been found, the association should not be considered more than a chance positional coincidence. Nevertheless as mentioned, there is a whole new class of objects that are now unidentified and that are close to energetic pulsars, that could potential belong to this class of objects.

4 Category C - Sources for which the multi-frequency data does not (yet) provide a consistent picture

The sources belonging to this class of objects have a good positional counterpart, but the multi-frequency data does not (yet) provide a consistent picture of the emission mechanism. One object of this class is HESS J1813–178. This slightly extended gamma-ray source was originally discovered in the H.E.S.S. Galactic plane survey and originally described as unidentified. Shortly afterwards several papers were published, describing the positional coincidence with an ASCA X-ray source (2-8 keV) [19], an Integral hard X-ray source (20-100 keV) [20], both having the same angular resolution and therefore like H.E.S.S. unable to resolve the object.

Finally VLA archival radio data (90 cm) were reported [19] showing a 2.5' diameter shell-like object coincident with the X-ray sources and with HESS J1813–178 (see Figure 3). This observation led to the conclusion that the positionally coincident object was a Supernova remnant and that the gamma-ray emission was either caused by the shell or by a centrally located PWN. However, the multi-frequency data does not distinguish between the two scenarios, due to the lack of spatial resolution of the X-ray and gamma-ray instruments. A preliminary analysis of a recent 30 ks XMM-Newton observation of the region point to a PWN origin of the emission, which would in turn allow to model the radio to

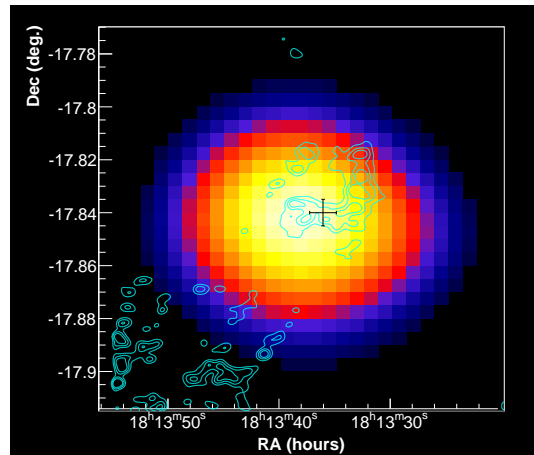


Fig. 3 Gamma-ray image of HESS J1813–178 overlaid with VLA 20 cm radio data in which the shell-type structure of the positional counterpart to the gamma-ray source can be seen. The best fit position of the gamma-ray excess is marked with a magenta cross.

gamma-ray data in the picture of a composite SNR and therefore finally possibly identifying HESS J1813–178 as a gamma-ray PWN. The example of HESS J1813–178 shows that high-quality multi-frequency are a prerequisite in the identification of a gamma-ray source and an ongoing programme is connected to the study of the unidentified gamma-ray sources with high-resolution X-ray detectors like Chandra, XMM-Newton and Suzaku. Other objects for which the multi-frequency data at this moment do not allow firm conclusions about potential counterparts are e.g. HESS J1640–465 and HESS J1834–087.

5 Category D - Sources with no counterpart

For this class of sources there is as of yet no counterpart at other wavelength determined. The common belief is, that this is due to insufficient (in terms of sensitivity) multi-wavelength data. In principle all new gamma-ray detections are first classified in this category, before they can be moved to another class with the help of MWL data. The most prominent examples of this class are the HEGRA source in the Cygnus region (TeV J2032+4131) [21] for which even in deep 50 ks Chandra observation no obvious X-ray counterpart was found. A similar case is the unidentified H.E.S.S. source HESS J1303–631 [22], serendipitously discovered in observations of the binary pulsar PSR B1259–63. Also here a Chandra observation did not reveal any obvious positional counterpart [23]. In the search for X-ray counterparts XMM-Newton seems to be best suited for the Galactic gamma-ray sources found by H.E.S.S. because the high sensitivity towards extended structures seems to be advantageous for the gamma-ray sources that typically have extensions of the order of 0.1° .

Table 2 Summary of the classes for the H.E.S.S. Galactic gamma-ray sources.

Source	Class	Comment
J1713–397	A	SNR RX J1713.7–3946
J0852–463	A	SNR RX J0852.0–4622
J0835–455	A	PWN Vela X
J1302–638	A	PWN PSR B1259–63
J1420–607	A	PWN PSR J1420–6048
J1514–591	A	PWN MSH 15–52
J1747–281	A	PWN G0.9+0.1
J1804–216	B	PWN or SNR?
J1825–137	B	PWN different scale
J1640–465	C	SNR?
J1813–178	C	Composite SNR?
J1834–087	C	SNR?
J1303–631	D	
J1614–518	D	
J1632–478	D	
J1634–472	D	
J1702–410	D	
J1708–420	D	
J1745–290	D	Galactic Centre source
J1745–303	D	
J1837–069	D	

A large fraction of the new H.E.S.S. sources can be categorised into this class. Examples are: HESS J1702–420, HESS J1708–410 or HESS J1745–303. As previously mentioned, there is an ongoing effort to investigate these sources with various instruments from radio to gamma-rays.

6 Summary and Conclusion

Table 2 summarises the H.E.S.S. gamma-ray sources into the proposed categories as given in table 1. As can be seen from this table, for less than half a firm counterpart can be identified, putting these sources into class A. The majority of the sources has to be classified as unidentified, since no good counterpart at other wavebands exists at all. It is evident, that the gathering of multi-waveband data will help in identifying these objects. It should however also be noted, that a positional coincidence alone does not help. A consistent modelling of the emission mechanisms at work in generating the gamma-rays must be invoked, before a firm association can be established. For the upcoming GLAST satellite, the situation will be further complicated by source confusion due to the larger point-spread function and also by the stronger diffuse gamma-ray background from decays of neutral pions in the Galactic plane.

The support of the Namibian authorities and of the University of Namibia in facilitating the construction and operation of H.E.S.S. is gratefully acknowledged, as is the support by the German Ministry for Education and Research (BMBF), the Max Planck Society, the French Ministry for Research, the CNRS-IN2P3 and the Astroparticle Interdisciplinary Programme of the CNRS,

the U.K. Particle Physics and Astronomy Research Council (PPARC), the IPNP of the Charles University, the South African Department of Science and Technology and National Research Foundation, and by the University of Namibia. We appreciate the excellent work of the technical support staff in Berlin, Durham, Hamburg, Heidelberg, Palaiseau, Paris, Saclay, and in Namibia in the construction and operation of the equipment.

References

- Aharonian, F. A., et al. (*H.E.S.S. Collaboration*): “A new population of very high energy γ -ray sources in the Milky Way”. *Science* **307**, 1938 (2005)
- Aharonian, F. A., et al. (*H.E.S.S. Collaboration*): The H.E.S.S. survey of the Inner Galaxy in very high-energy gamma-rays. *ApJ* **636**, 777 (2006)
- Hartman, R. C., et al.: The Third EGRET Catalog of High-Energy Gamma-Ray Sources. *ApJS* **123**, 79 (1999)
- Aharonian, F. A., et al. (*H.E.S.S. Collaboration*): Observations of the Crab Nebula with H.E.S.S.. *A&A* in press (2006) astro-ph/0607333
- Aharonian, F. A., et al. (*H.E.S.S. Collaboration*): Discovery of very high energy gamma rays associated with an X-ray binary. *Science* **309**, 746 (2005)
- Aharonian, F. A., et al. (*H.E.S.S. Collaboration*): Discovery of Orbital modulation in the very high energy gamma-ray emission from the X-ray binary LS 5039. *A&A* in press (2006)
- Albert, J. et al.: Variable Very High Energy Gamma-ray Emission from the Microquasar LS I +61 303, *Science* **312** 1771 (2006)
- Aharonian, F., et al. (*H.E.S.S. Collaboration*): Very high energy gamma rays from the composite SNR G0.9+0.1. *A&A* **432**, 25 (2005)
- Aharonian, F., et al. (*H.E.S.S. Collaboration*): High-energy particle acceleration in the shell of a supernova remnant. *Nature* **432**, 75 (2004)
- Aharonian, F. A., et al. (*H.E.S.S. Collaboration*): A detailed spectral and morphological study of the γ -ray supernova remnant RX J1713.7–3946. *A&A* **449**, 223 (2006)
- Aharonian, F., et al. (*H.E.S.S. Collaboration*): Detection of TeV γ -ray emission from the shell-type supernova remnant RX J0852.0–4622 with H.E.S.S.. *A&A*, **437**, L7 (2005)
- Aharonian, F. A., et al. (*H.E.S.S. Collaboration*): Discovery of extended VHE gamma-ray emission from the asymmetric pulsar wind nebula in MSH 15–52 with HESS. *A&A* **435**, L17 (2005)
- Aharonian, F. A., et al. (*H.E.S.S. Collaboration*): First detection of a VHE gamma-ray spectral maximum from a Cosmic source: H.E.S.S. discovery of the Vela X nebula. *A&A*, **448**, L43 (2006).
- Blondin, J.M., Chevalier, R.A., & Frierson, D.M.: Pulsar wind nebulae in evolved supernova remnants. *ApJ* **563**, 806 (2001)
- Aharonian, F. A., et al. (*H.E.S.S. Collaboration*): A possible association of the new VHE γ -ray source HESS J1825–137 with the pulsar wind nebula G 18.0–0.7. *A&A* **442**, L25 (2005)
- Aharonian, F. A., et al. (*H.E.S.S. Collaboration*): Energy dependent γ -ray morphology in the Pulsar wind nebula HESS J1825–137. *A&A* accepted for publication (2006) astro-ph/0607548
- Gaensler, B. M., Schulz, N. S., Kaspi, V. M. Pivovarov, M. J., & Becker, W. E.: XMM-Newton Observations of PSR B1823–13: An asymmetric synchrotron nebula around a vela-like pulsar. *ApJ* **588**, 441 (2003)

18. Lemière, A., for the H.E.S.S. Collaboration, To appear in the Proceedings of the 29th ICRC, Pune (2005)
19. Brogan, C. L., Gaensler, B. M., Gelfand, J. D., Lazendic, J. S., Lazio, T. J., Kassim, N. E., & McClure-Griffiths, N. M.: Discovery of a radio supernova remnant and non-thermal X-rays coincident with the TeV source HESS J1813-178. **629** L105 (2005)
20. Ubertini, P. et al.: Integral IGR J18135–1751== HESS J1813–178: A new cosmic high energy accelerator from KeV to TeV. *ApJL* **629**, L109 (2005).
21. Aharonian, F., et al.: The unidentified TeV source (TeV J2032+4130) and surrounding field: Final HEGRA IACT-System results. *A&A*, **431**, 197A (2005)
22. Aharonian, F., et al. (*H.E.S.S. Collaboration*): Serendipitous discovery of the unidentified extended TeV γ -ray source HESS J1303–631. *A&A* **439**, 1013 (2005)
23. Mukherjee, R., Halpern, J. P.: Chandra Observation of the Unidentified TeV Gamma-Ray Source HESS J1303-631 in the Galactic Plane. *ApJ* **629** 1017 (2005)